

# ornl

ORNL/TM-11404

**OAK RIDGE  
NATIONAL  
LABORATORY**

**MARTIN MARIETTA**

MARTIN MARIETTA ENERGY SYSTEMS LIBRARIES



3 4456 0328528 2

**Preliminary Cross Sections for  
Gamma Rays Produced by Interaction  
of 1 to 40 MeV Neutrons with  $^{59}\text{Co}$**

T. E. Slusarchyk

OPERATED BY  
MARTIN MARIETTA ENERGY SYSTEMS, INC.  
FOR THE UNITED STATES  
DEPARTMENT OF ENERGY

This report has been reproduced directly from the best available copy.

Available to DOE and ORES contractors from the Office of Scientific and Technical Information, P.O. Box 60, Oak Ridge, TN 37831; prices available from (615) 576 8401. NTIS price code:

Available to the public from the National Technical Information Service, U.S. Department of Commerce, 5235 Port Royal Rd., Springfield, VA 22161.  
NTIS price code - Printed Copy - A034304-4 A01

This report was prepared as an account of work sponsored by an agency of the United States Government. Neither the United States Government nor any agency thereof, nor any of their employees, makes any warranty, express or implied, or assumes any legal liability or responsibility for the accuracy, completeness, or usefulness of any information, apparatus, product, or process disclosed, or represents that its use should not infringe on privately owned rights. Reference herein to any specific commercial product, process, or service by trade name, trademark, manufacturer, or otherwise, does not necessarily constitute or imply its endorsement, recommendation, or favoring by the United States Government or any agency thereof. The views and opinions of authors expressed herein do not necessarily state or reflect those of the United States Government or any agency thereof.

Engineering Physics and Mathematics

**PRELIMINARY CROSS SECTIONS FOR  
GAMMA RAYS PRODUCED BY INTERACTION  
OF 1 TO 40 MeV NEUTRONS WITH  $^{59}\text{Co}$**

Thomas E. Slusarchyk\*

DATE PUBLISHED — October 15, 1989

\*Consultant, U. S. Navy

Prepared for the  
Office of Energy Research,  
Nuclear Physics

**NOTICE:** This document contains information of a preliminary nature. It is subject to revision or correction and therefore does not represent a final report.

Prepared by the  
OAK RIDGE NATIONAL LABORATORY  
Oak Ridge, Tennessee 37831  
operated by  
MARTIN MARIETTA ENERGY SYSTEMS, INC.  
for the  
U.S. DEPARTMENT OF ENERGY  
under contract DE-AC05-84OR21400





## CONTENTS

ABSTRACT . . . . .	v
1. INTRODUCTION . . . . .	1
2. EXPERIMENTAL DETAILS . . . . .	2
3. RESULTS . . . . .	7
4. CONCLUDING REMARKS . . . . .	24
REFERENCES . . . . .	25



## ABSTRACT

Data for 46 distinct gamma rays previously obtained at the 20-meter station of the Oak Ridge Electron Linear Accelerator (ORELA) were studied to determine cross sections for 1.0–40.0 MeV neutron interactions with  $^{59}\text{Co}$ . Data reduction methods and preliminary cross sections are given in this report.



# 1. INTRODUCTION

The use of stainless steel containing  $^{59}\text{Co}$  in accelerators and reactors exposes it to fluences of high-energy neutrons. Cross-section data from  $^{59}\text{Co}$  would give engineers needed information which would be used in determining the amount of shielding necessary to attenuate the gamma rays to a safe level.

In an attempt to obtain accurate cross section data for  $^{59}\text{Co}$ , D. C. Larson and J. K. Dickens conducted a series of experiments using the Oak Ridge Electron Linear Accelerator (ORELA) at Oak Ridge National Laboratory (ORNL) for neutron energies of 1.0–40.0 MeV. The present document reports on one aspect of determining the cross section, that is, determining the yield, and the resultant conversion to (uncorrected) cross section  $\sigma$ .

The reduction of data is formulated as follows:

$$\sigma = (Y/Eff)/[(N_n) * (N_s)]$$

where

- $\sigma$  = cross section for production of a gamma ray having energy  $E_\gamma$  by neutrons having energies in a given energy bin ( $E_n$  low to  $E_n$  high)
- $Y$  = yield (in counts) of the peak in a spectrum corresponding to the gamma-ray energy  $E_\gamma$
- $Eff$  = efficiency of the recording gamma-ray detector for detection of the gamma ray having energy  $E_\gamma$
- $N_n$  = number of neutrons (flux) in the energy bin ( $E_n$  low to  $E_n$  high)
- $N_s$  = number of scatterers (number of atoms of  $^{59}\text{Co}$ )

The following reactions were observed and are listed with their reaction  $Q$ -values:

REACTION	Q-VALUE (MeV)
$^{59}\text{Co}(n, n')^{59}\text{Co}$	- 1.099
$^{59}\text{Co}(n, 2n)^{58}\text{Co}$	-10.454
$^{59}\text{Co}(n, 3n)^{57}\text{Co}$	-19.027
$^{59}\text{Co}(n, p)^{59}\text{Fe}$	- 0.783
$^{59}\text{Co}(n, np)^{58}\text{Fe}$	- 7.364
$^{59}\text{Co}(n, 2np)^{57}\text{Fe}$	-17.408
$^{59}\text{Co}(n, ^4\text{He})^{56}\text{Mn}$	+ 0.329
$^{59}\text{Co}(n, n^4\text{He})^{55}\text{Mn}$	- 6.941

## 2. EXPERIMENTAL DETAILS

A general schematic of the experiment is shown in Figure 1, and a discussion of it is found in references 1 and 2. The sample of cobalt was 100%  $^{59}\text{Co}$  and was disk-shaped with a 10.16-cm diameter and a 0.2032-cm thickness. It had a mass of 149 grams. The neutron beam had a diameter of 7.34 cm. Flux measurements were made using an NE-110 plastic scintillator. To obtain cross section data, an intrinsic Ge detector was placed at an angle of 125 degrees with respect to the incident neutron beam. The dividing of the neutrons into energy bins was accomplished by time-of-flight calculations.

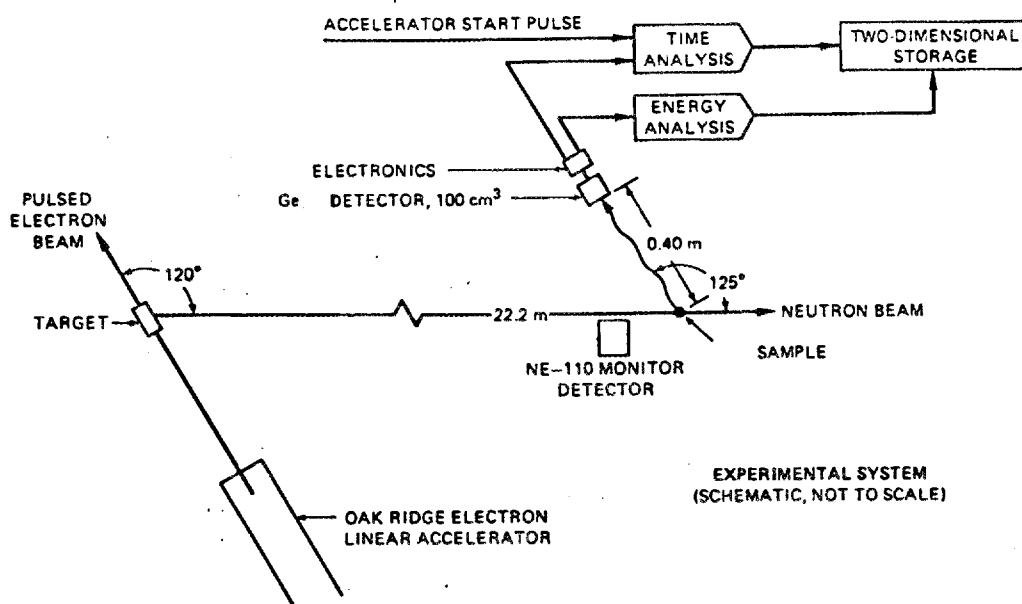
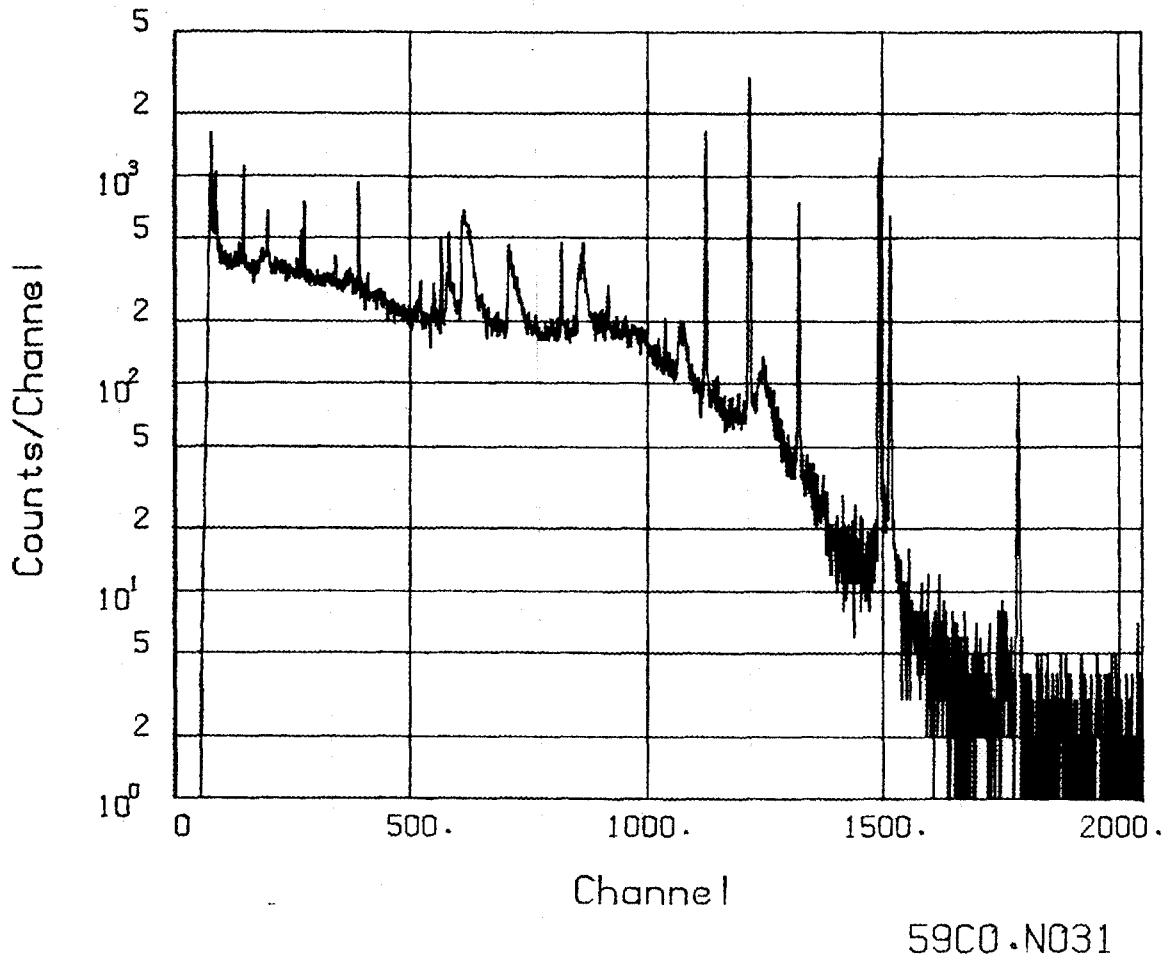


Fig. 1. Schematic representation of the experimental station. Starting from the lower left of this figure, 140-MeV electrons produced by the Oak Ridge Electron Linear Accelerator (ORELA) impinged upon a tantalum target (not shown separately) producing Bremsstrahlung. Neutrons produced in the Be by subsequent photonuclear reactions were guided to the experimental area by an evacuated, 20-m-long flight tube located at 120 degrees with respect to the incident electron beam. Collimators were inserted into the flight tube to define the neutron beam to a diameter of 7.3 cm at the sample position. The beam traveled approximately 2 m in air before impinging on the  $^{59}\text{Co}$  sample. A small NE-110 scintillator intercepted approximately 1% of the incident neutron flux and was used as a beam monitor. Two types of pulses were extracted from the detector electronics. One was for energy analysis using standard very high resolution pulse-amplitude analyzing equipment (3-microsec time constants for the spectroscopy amplifier). The other pulse was used for fast-timing analysis to determine the flight time of the neutron responsible for the detected gamma ray. The time-of-flight datum was correlated with the energy datum in a data-acquisition computer, which sorted and then stored events on a bulk storage disk pack.

Altogether, 38 4096-channel gamma-ray spectra corresponding to 38 neutron time-of-flight bins for  $E_n$  between threshold and 38 MeV were studied to provide cross-section data. Plots of these spectra were made in order to find out which reactions were most prolific. One of these spectra is shown in Figure 2.



**Fig. 2. Pulse height spectrum for 1.64–1.95-MeV neutrons interacting with the cobalt sample.** Starting from channel 1100 and reading to the right, six narrow  $^{59}\text{Co}$  peaks are clearly visible. They are (respectively) 1098.9 keV, 1190.0 keV, 1291.3 keV, 1458.8 keV, 1481.8 keV, and 1744.5 keV. Neutron inelastic interactions with Ge in the detector cause the broad peaks. The experimental dispersion is approximately 0.9 keV/channel.

A combination of data-reduction techniques involving computer and manual methods was used to obtain the cross-section results. The computer analysis of the data was undertaken using the GRPGLI<sup>3</sup> computer code which locates the gamma-ray peaks in the spectra, determines the centroid and uncertainty of each peak, determines the cross sections, and attempts to identify the reaction from which the gamma ray came.

#### 4 EXPERIMENTAL DETAILS

One problem encountered with the use of the GRPGLI was the splitting of one large peak into two or more smaller peaks and then selecting just one of the smaller peak's area to calculate the cross section. These were the most obvious corrections that needed to be made. In these cases, the program PLOTPACK<sup>4</sup> was used to force new limits of integration that included both smaller peaks. Figure 3 is an example of a double peak that should have been analyzed as a single, large peak.

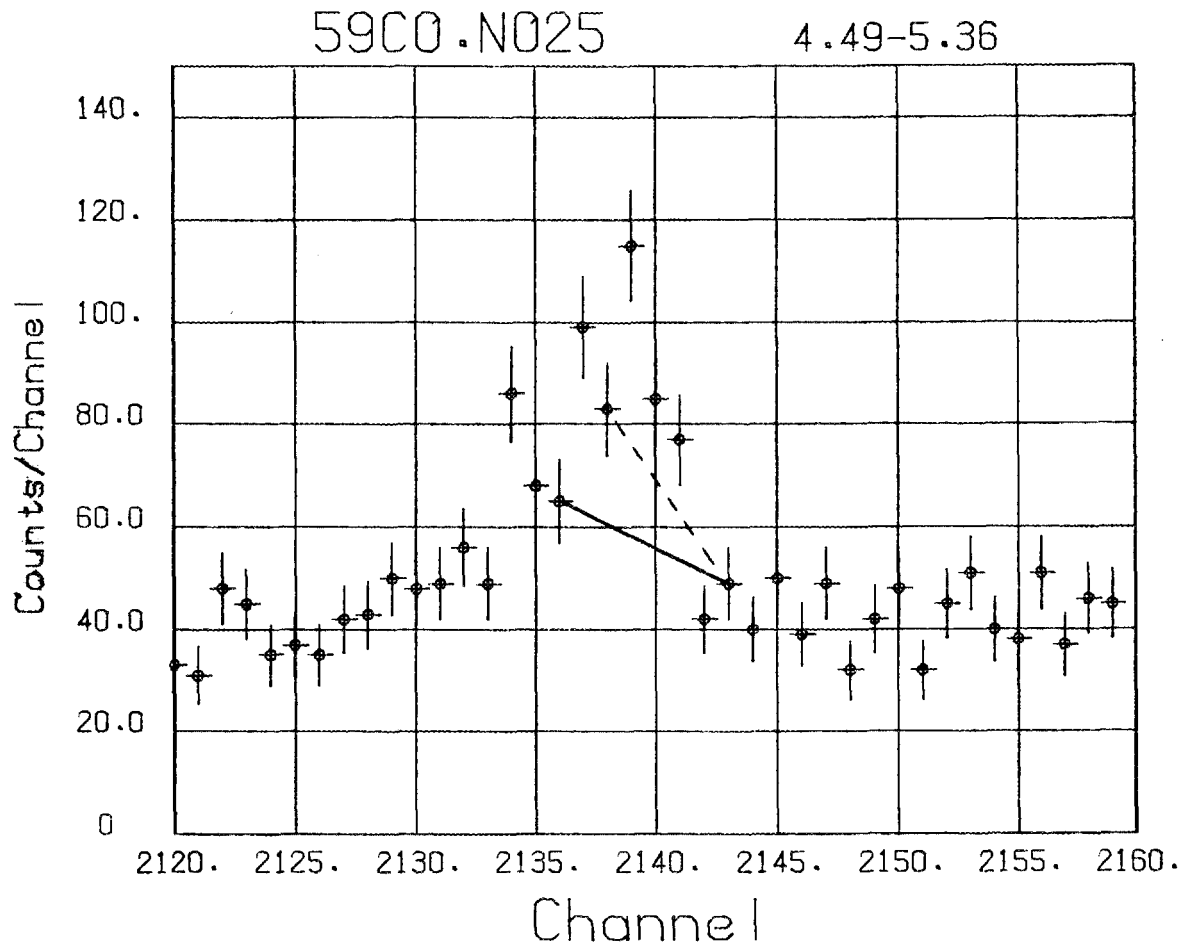


Fig. 3. Portion of a spectrum showing the 2087.2-keV gamma-ray peak from the  $^{59}\text{Co}(n, n')^{59}\text{Co}$  reaction. The dashed line represents the background for this peak the GRPGLI code reported while the solid line represents the corrected background obtained through the use of PLOTPACK. The gamma-ray centroid should be located at channel 2140. For this spectrum, the incident neutrons ranged in energy from 4.49 MeV to 5.36 MeV.

Another problem with the GRPGLI code was locating peaks and computing cross sections for gamma rays that were not sufficiently above the background radiation. When these gamma rays were viewed by the use of the PLOTPACK program, it was decided in many cases that the existence of the gamma ray was doubtful. In these cases, the computed cross sections were omitted. Occasionally, the GRPGLI code identified "peaks" for gamma rays below the reaction thresholds. These were also omitted.

Sometimes, the close proximity of a neighboring gamma ray to the area where the computer program was searching for a peak caused the computer to find a peak. The computer would integrate part of this adjacent peak so that the centroid would remain close enough to the channel where it was searching. The computer then reported it. After inspection with the use of PLOTPACK, the reported cross sections were omitted if it was determined that the real peak was off by more than 1.5 channels. Figure 4 shows an example of the computer integrating part of a peak that is close to the channel it is searching for a gamma ray.

Overall, the computer program GRPGLI did most of the work of integrating and determining cross sections. It would have been a tremendously time-consuming process to check each of the 46 gamma rays at all incident energies to be absolutely sure the code found the correct peak. Therefore, most of the cross sections rely on the accuracies of the GRPGLI.

6 EXPERIMENTAL DETAILS

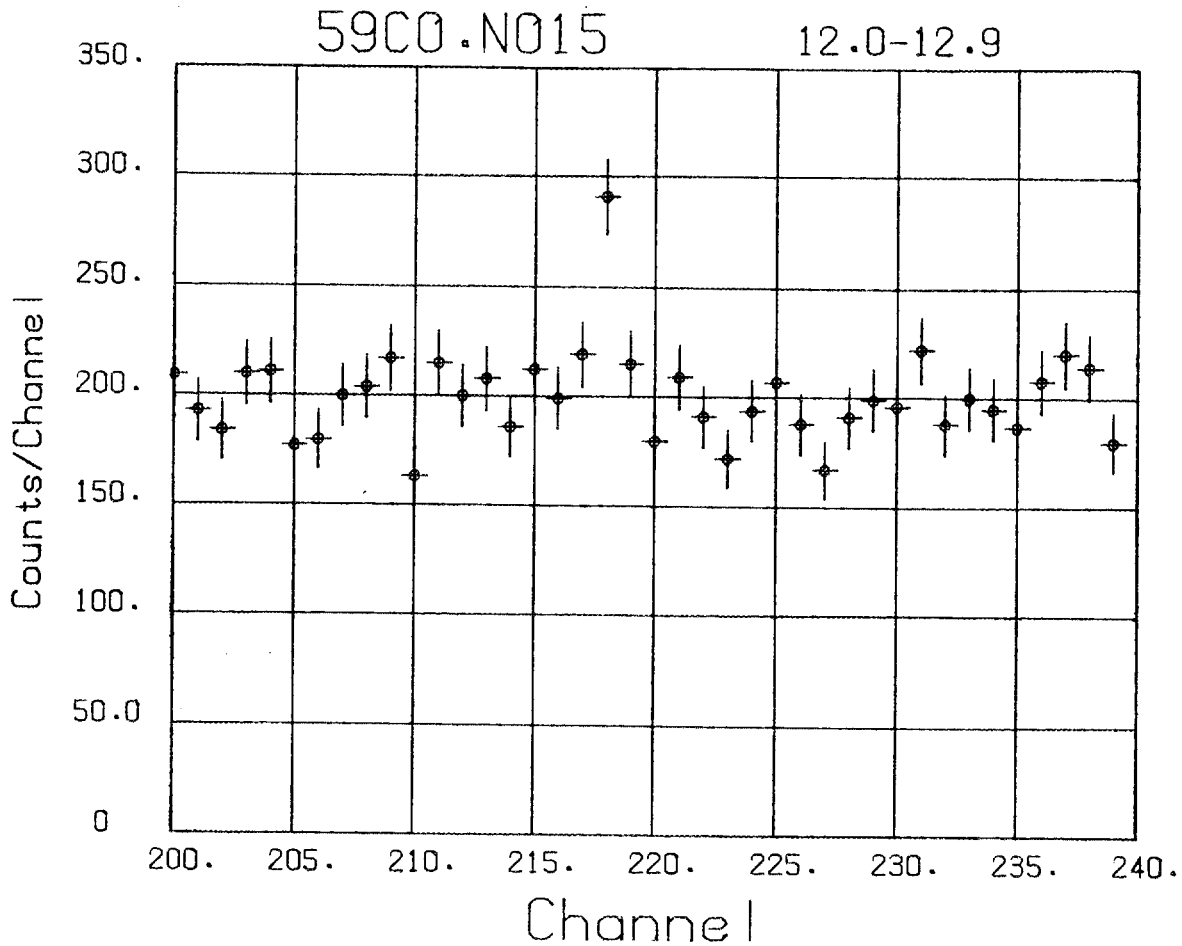


Fig. 4. Portion of a spectrum showing a peak close where the 212.0-keV gamma ray should appear from the  $^{59}\text{Co}(n, ^4\text{He})^{56}\text{Mn}$  reaction. The corresponding channel for the 212.0-keV peak is 216.3. The centroid of this peak is located at channel 218.0 according to the GRPGLI code and the PLOTPACK. It was determined that this was too far off to be the 212.0-keV gamma ray emanating from  $^{56}\text{Mn}$  and must be coming from some other source. The cross section the GRPGLI computed was omitted. For this spectrum, the incident neutrons ranged in energy from 12.0 MeV to 12.9 MeV.

### 3. RESULTS

Tables 1-8 contain preliminary cross sections for various gamma rays observed as a function of incident neutron energy.

Corrections for gamma-ray attenuation in the sample are already included in the cross-section results listed above. The attenuation correction had the most pronounced effect on the lower energy gamma rays. For the lowest energy gamma ray reported (122.0 keV), the correction was approximately 40%. For gamma rays above 2,000 keV, the correction amounted to less than 5%.

Multiple-scattering corrections have not been included in these results. These corrections require the use of an iterative Monte-Carlo technique. Additionally, corrections for electronic timing "walk" variations have not been made. These variations have the largest effect at lowest energies ( $E_\gamma < 400$  keV). It is estimated that the maximum error due to excluding these corrections to the calculations is 5%.

The most prolific reaction by far was the  $^{59}\text{Co}(n,n')^{59}\text{Co}$  followed by the  $^{59}\text{Co}(n,2n)^{58}\text{Co}$  reaction. In general, the gamma-ray cross sections appeared after the incident neutron energies exceeded the reaction Q-value, increased to a maximum, and then died out as the neutron energies increased far beyond the reaction threshold. Typical plots for each reaction observed are shown in Figures 5-12. The gamma rays in these figures were chosen because of their large cross sections.

It is interesting to note that although the (n,n'), the (n,2n) and the (n,3n) reactions began to appear when the incident neutron energies just exceeded the reaction Q-value, the reactions involving protons and alpha particles did not appear until the incident neutron energies were much higher than their reaction Q-value. This extra energy is used to break the charged particle through the Coulomb barrier present around the nucleus. For the proton, the barrier potential ranged from 3-8 MeV, while for the alpha particle, the barrier potential ranged from 8-13 MeV.

Table 1. Measured cross sections (in mb) for production of gamma rays following neutron interactions with  $^{59}\text{Co}$ 

$E_n$ (MeV)	Gamma-ray energy (keV)					
	1098.9	1190.0	1291.3	142.8	1458.8	1482.1
1.13- 1.22	41.0 ± 1.9	11.0 ± 0.9				
1.22- 1.35	59.4 ± 2.4	123.3 ± 4.1	5.15 ± 0.57			
1.35- 1.64	86.8 ± 2.6	212.1 ± 5.5	41.1 ± 1.4	6.99 ± 0.75	40.7 ± 1.5	18.0 ± 0.9
1.64- 1.95	121.2 ± 3.2	262.5 ± 6.2	66.8 ± 2.0	12.0 ± 1.0	125.4 ± 3.4	67.6 ± 2.1
1.95- 2.28	128.7 ± 3.4	300.9 ± 7.3	81.1 ± 2.6	16.1 ± 1.2	151.7 ± 4.0	92.4 ± 2.8
2.28- 2.58	135.8 ± 3.8	343.6 ± 8.3	106.8 ± 3.4	15.1 ± 1.5	173.4 ± 4.9	115.3 ± 3.8
2.58- 2.81	130.8 ± 5.1	350.0 ± 11.5	109.6 ± 4.9	16.1 ± 2.4	168.5 ± 7.2	103.5 ± 5.1
2.81- 3.67	127.0 ± 3.8	371.3 ± 10.0	117.5 ± 3.6	17.3 ± 1.5	181.4 ± 5.3	115.3 ± 3.8
3.67- 4.49	145.4 ± 4.5	373.5 ± 10.7	96.4 ± 3.6	15.3 ± 1.8	206.0 ± 6.6	119.6 ± 4.2
4.49- 5.36	146.5 ± 5.8	394.8 ± 14.3	91.7 ± 4.3	16.7 ± 2.0	227.1 ± 8.9	118.9 ± 5.1
5.36- 6.19	131.9 ± 4.9	386.3 ± 13.0	86.2 ± 3.6	18.9 ± 2.3	222.8 ± 8.5	98.6 ± 4.5
6.19- 7.04	124.2 ± 5.8	337.2 ± 14.5	82.8 ± 4.3	16.8 ± 2.4	239.8 ± 10.8	85.0 ± 4.7
7.04- 7.75	108.8 ± 6.8	311.6 ± 16.6	79.6 ± 5.5	14.4 ± 0.3	235.5 ± 13.2	72.9 ± 5.1
7.75- 8.44	114.0 ± 7.5	341.4 ± 20.1	77.9 ± 5.3	10.5 ± 2.8	250.4 ± 15.1	84.4 ± 5.9
8.44- 9.23	101.3 ± 5.8	309.4 ± 16.0	73.2 ± 4.5	12.4 ± 2.7	258.9 ± 13.8	76.7 ± 5.3
9.23- 9.82	100.7 ± 6.2	337.2 ± 17.7	74.9 ± 5.1	8.7 ± 3.2	244.0 ± 14.0	75.9 ± 5.5
9.82-10.4	105.8 ± 6.8	328.6 ± 18.6	71.1 ± 5.7	9.7 ± 3.2	295.0 ± 16.8	76.5 ± 5.5
10.4 -11.1	88.1 ± 6.0	288.1 ± 17.5	53.4 ± 4.9	4.4 ± 3.0	273.7 ± 16.8	70.2 ± 5.3
11.1 -12.0	68.6 ± 4.5	273.2 ± 14.1	47.5 ± 3.4	5.1 ± 3.0	248.3 ± 12.9	63.8 ± 5.3
12.0 -12.9	64.8 ± 4.3	219.8 ± 11.3	34.3 ± 3.6	4.8 ± 2.9	201.2 ± 10.8	49.8 ± 3.8
12.9 -13.8	55.8 ± 4.1	160.1 ± 10.0	26.8 ± 3.2	6.2 ± 3.0	168.5 ± 10.2	33.1 ± 4.0
13.8 -15.2	32.9 ± 2.4	113.1 ± 7.0	17.6 ± 3.6	3.5 ± 2.8	102.1 ± 6.6	22.3 ± 2.3
15.2 -16.9	23.5 ± 3.2	87.3 ± 6.0	16.1 ± 1.6	7.3 ± 2.9	71.3 ± 5.3	16.9 ± 1.9
16.9 -18.8	27.6 ± 4.7	65.5 ± 6.0	11.9 ± 3.8		65.1 ± 5.5	5.5 ± 3.6
18.8 -20.5	19.9 ± 2.8	59.1 ± 7.0	10.4 ± 4.3		63.0 ± 7.0	7.4 ± 4.4
20.5 -22.5	20.7 ± 2.8	60.6 ± 5.8	5.7 ± 4.0		45.6 ± 4.9	10.1 ± 4.5
22.5 -24.9	22.2 ± 5.6	50.1 ± 5.5	6.4 ± 4.5		26.1 ± 4.0	11.9 ± 4.4
24.9 -26.9	19.5 ± 6.2	24.6 ± 4.9	8.2 ± 4.9		36.7 ± 5.9	
26.9 -29.1	15.6 ± 6.4	63.8 ± 6.2			30.3 ± 4.2	
29.1 -31.7		41.8 ± 6.8			24.0 ± 5.5	
31.7 -33.6		32.7 ± 6.4			34.0 ± 6.6	
33.6 -35.7		22.8 ± 11.5			31.4 ± 7.2	
35.7 -38.0		44.2 ± 10.2			32.7 ± 8.1	

Table 2. Measured cross sections (in mb) for production of gamma rays following neutron interactions with  $^{59}\text{Co}$

$E_n$ (MeV)	Gamma-ray energy (keV)					
	1744.8	580.0	2087.2	993.1	723.5	650.7
1.64- 1.95	13.7 ± 0.9					
1.95- 2.28	45.6 ± 1.9	8.83 ± 0.52	3.35 ± 0.69	3.0 ± 1.4	2.0 ± 1.5	
2.28- 2.58	52.4 ± 2.5	27.5 ± 1.1	19.7 ± 1.6	44.6 ± 1.7	16.2 ± 0.9	7.91 ± 0.76
2.58- 2.81	62.1 ± 3.6	32.6 ± 1.7	22.5 ± 2.3	53.2 ± 3.0	17.4 ± 1.4	19.3 ± 1.4
2.81- 3.67	65.4 ± 2.7	35.0 ± 1.3	30.1 ± 1.7	60.9 ± 2.1	25.8 ± 1.1	23.7 ± 0.9
3.67- 4.49	62.9 ± 3.0	28.6 ± 1.1	28.6 ± 1.9	59.4 ± 2.1	21.9 ± 1.5	26.1 ± 1.7
4.49- 5.36	64.0 ± 3.4	34.5 ± 2.2	23.0 ± 2.5	72.1 ± 3.2	23.7 ± 1.3	24.8 ± 1.3
5.36- 6.19	59.1 ± 3.4	25.4 ± 1.3	15.3 ± 2.1	74.7 ± 3.2	17.6 ± 1.1	20.7 ± 1.2
6.19- 7.04	60.2 ± 3.6	28.9 ± 1.5	18.4 ± 2.8	69.1 ± 3.4	18.1 ± 1.2	21.8 ± 1.5
7.04- 7.75	57.0 ± 4.0	21.4 ± 1.6	17.1 ± 1.9	67.4 ± 4.1	15.8 ± 1.3	24.0 ± 4.8
7.75- 8.44	48.3 ± 5.3	25.4 ± 2.0	12.5 ± 1.7	76.8 ± 5.2	15.3 ± 2.6	23.7 ± 2.0
8.44- 9.23	48.1 ± 3.6	24.3 ± 1.7	16.9 ± 2.0	76.0 ± 4.5	12.6 ± 1.3	24.0 ± 2.0
9.23- 9.82	51.3 ± 5.1	20.7 ± 1.9	13.6 ± 4.4	78.8 ± 5.2	16.4 ± 1.7	17.8 ± 5.5
9.82-10.4	56.6 ± 4.6	23.0 ± 3.1	14.8 ± 4.4	85.8 ± 5.6	11.3 ± 4.4	22.7 ± 2.0
10.4 -11.1	61.9 ± 5.1	14.4 ± 4.2	13.4 ± 4.2	80.7 ± 5.6	9.8 ± 4.3	19.6 ± 1.9
11.1 -12.0	26.2 ± 5.1	10.8 ± 4.2	8.0 ± 4.3	71.0 ± 5.2	6.4 ± 4.2	16.4 ± 1.6
12.0 -12.9	28.5 ± 2.5	9.3 ± 4.2	4.4 ± 3.9	54.9 ± 3.6	6.7 ± 4.0	19.1 ± 1.7
12.9 -13.8	25.1 ± 3.2	7.5 ± 3.9	8.0 ± 3.5	42.5 ± 4.5	4.9 ± 3.9	9.3 ± 2.6
13.8 -15.2	10.6 ± 3.3	7.4 ± 3.4		26.8 ± 3.2		
15.2 -16.9	10.2 ± 3.3			13.0 ± 3.3		
16.9 -18.8	12.0 ± 1.9			18.9 ± 3.9		
18.8 -20.5	11.1 ± 4.1			16.0 ± 4.9		
20.5 -22.5	8.3 ± 4.7			21.1 ± 4.9		
22.5 -24.9	8.6 ± 4.4			16.5 ± 4.8		
24.9 -26.9	10.6 ± 4.5			18.3 ± 3.0		
26.9 -29.1	7.4 ± 5.4			11.5 ± 5.7		
29.1 -31.7	6.5 ± 5.1			12.3 ± 8.3		
31.7 -33.6				9.7 ± 9.6		

Table 3. Measured cross sections (in mb) for production of gamma rays following neutron interactions with  $^{59}\text{Co}$ 

$E_n$ (MeV)	Gamma-ray energy (keV)					
	2478.2	2540.4	2583.2	2781.2	2825.1	2910.1
2.28- 2.58	$1.49 \pm 0.63$					
2.58- 2.81	$10.7 \pm 2.0$	$3.9 \pm 1.3$	$2.7 \pm 1.3$			
2.81- 3.67	$19.0 \pm 1.5$	$7.0 \pm 1.0$	$14.4 \pm 1.4$	$2.1 \pm 1.1$	$7.8 \pm 1.2$	$2.99 \pm 0.50$
3.67- 4.49	$10.9 \pm 1.6$	$7.1 \pm 1.3$	$11.2 \pm 1.7$	$2.5 \pm 1.5$	$12.1 \pm 1.4$	$3.60 \pm 0.98$
4.49- 5.36	$6.3 \pm 1.7$	$10.0 \pm 1.8$	$10.0 \pm 1.8$	$4.2 \pm 1.5$	$8.9 \pm 1.8$	$3.1 \pm 1.5$
5.36- 6.19	$10.3 \pm 1.2$	$6.0 \pm 2.2$	$9.7 \pm 1.2$	$2.9 \pm 2.1$	$7.9 \pm 2.2$	$2.5 \pm 2.0$
6.19- 7.04	$10.4 \pm 2.6$	$7.1 \pm 2.4$	$5.5 \pm 2.3$	$3.9 \pm 2.3$	$5.7 \pm 2.3$	
7.04- 7.75	$8.8 \pm 3.1$	$3.8 \pm 2.5$	$5.0 \pm 2.7$	$4.8 \pm 4.4$		
7.75- 8.44	$9.9 \pm 3.3$	$6.7 \pm 3.8$	$10.3 \pm 3.3$			
8.44- 9.23	$12.1 \pm 3.5$		$3.9 \pm 3.4$			
9.23- 9.82	$7.4 \pm 4.5$		$6.3 \pm 3.9$			
9.82-10.4	$5.9 \pm 4.2$					
10.4 -11.1	$7.3 \pm 4.4$					

Table 4. Measured cross sections (in mb) for production of gamma rays following neutron interactions with  $^{59}\text{Co}$

$E_n$ (MeV)	Gamma-ray energy (keV)					
	2963.6	1720.1	522.4	1003.6	3275.4	1922.4
2.81-3.67	$1.36 \pm 0.65$	$1.6 \pm 1.2$	$2.4 \pm 1.5$	$11.1 \pm 1.8$	$1.49 \pm 0.56$	$1.69 \pm 0.93$
3.67-4.49	$5.97 \pm 0.92$	$4.6 \pm 1.7$	$6.2 \pm 1.9$	$13.0 \pm 1.6$	$6.1 \pm 1.1$	$6.7 \pm 1.3$
4.49-5.36	$3.9 \pm 1.6$	$4.5 \pm 2.1$	$4.9 \pm 2.1$	$8.37 \pm 0.75$	$5.6 \pm 1.6$	$5.34 \pm 0.70$
5.36-6.19			$8.3 \pm 2.3$			$4.9 \pm 1.5$
6.19-7.04			$7.95 \pm 0.68$			$5.8 \pm 2.4$
7.04-7.75			$3.4 \pm 2.8$			$5.0 \pm 3.0$
7.75-8.44			$3.4 \pm 3.1$			$8.5 \pm 3.1$
8.44-9.23			$4.2 \pm 3.1$			$6.5 \pm 3.1$
9.23-9.82			$3.9 \pm 3.8$			$7.7 \pm 3.5$

Table 5. Measured cross sections (in mb) for production of gamma rays following neutron interactions with  $^{59}\text{Co}$ 

$E_n$ (MeV)	Gamma-ray energy (keV)					
	365.7	321.0	349.1	432.7	774.2	1049.4
10.4-11.1	$4.4 \pm 3.6$	$5.1 \pm 3.4$				
11.1-12.0	$5.5 \pm 3.6$	$15.6 \pm 3.7$		$5.1 \pm 3.6$		$7.4 \pm 4.3$
12.0-12.9	$21.2 \pm 3.9$	$37.0 \pm 4.3$	$4.5 \pm 3.6$	$15.0 \pm 3.6$		$13.6 \pm 4.7$
12.9-13.8	$19.7 \pm 3.7$	$38.1 \pm 3.8$	$8.1 \pm 3.5$	$30.3 \pm 3.8$		$32.7 \pm 3.0$
13.8-15.2	$24.8 \pm 3.4$	$98.5 \pm 5.2$	$11.5 \pm 3.1$	$54.0 \pm 2.9$	$15.4 \pm 1.7$	$26.3 \pm 4.7$
15.2-16.9	$33.3 \pm 3.6$	$59.5 \pm 4.1$	$9.6 \pm 2.4$	$65.8 \pm 3.1$	$20.4 \pm 1.8$	$89.6 \pm 4.7$
16.9-18.8	$40.2 \pm 4.5$	$69.5 \pm 5.6$	$18.2 \pm 3.5$	$69.5 \pm 4.6$	$19.2 \pm 2.1$	$115.9 \pm 7.1$
18.8-20.5	$33.5 \pm 4.7$	$72.4 \pm 7.0$	$15.0 \pm 4.1$	$68.6 \pm 6.0$	$17.0 \pm 2.3$	$98.6 \pm 9.8$
20.5-22.5	$27.0 \pm 4.5$	$127.0 \pm 8.8$	$14.8 \pm 4.2$	$58.9 \pm 4.4$	$21.4 \pm 5.1$	$115.1 \pm 8.3$
22.5-24.9	$22.3 \pm 4.5$	$102.2 \pm 5.2$		$54.7 \pm 3.5$	$13.9 \pm 3.1$	$86.2 \pm 7.5$
24.9-26.9	$19.1 \pm 4.9$	$81.2 \pm 5.0$		$23.5 \pm 5.5$	$7.4 \pm 5.4$	$61.4 \pm 7.5$
26.9-29.1	$23.2 \pm 5.8$	$63.6 \pm 7.4$		$26.1 \pm 2.7$		$41.9 \pm 5.1$
29.1-31.7	$14.4 \pm 5.5$	$44.9 \pm 4.5$		$21.5 \pm 10.1$		$45.6 \pm 6.2$
31.7-33.6	$13.9 \pm 6.8$	$35.9 \pm 5.2$		$20.4 \pm 10.1$		$26.7 \pm 12.8$
33.6-35.7	$14.1 \pm 7.0$	$24.1 \pm 8.3$		$23.5 \pm 8.2$		$16.8 \pm 7.8$
35.7-38.0	$11.9 \pm 7.3$	$28.6 \pm 5.0$		$10.3 \pm 7.3$		

Table 6. Measured cross sections (in mb) for production of gamma rays following neutron interactions with  $^{59}\text{Co}$

$E_n$ (MeV)	Gamma-ray energy (keV)					
	727.3	1236.9	894.8	1050.8	1524.6	1555.3
11.1-12.0				7.0 ± 4.3		
12.0-12.9				12.2 ± 4.7		
12.9-13.8	10.1 ± 3.9			22.7 ± 3.0		
13.8-15.2	16.3 ± 1.6	7.7 ± 3.5	10.1 ± 3.8	56.9 ± 4.7	3.7 ± 2.9	
15.2-16.9	23.0 ± 2.8	8.0 ± 4.6	13.5 ± 3.8	89.6 ± 4.7	8.0 ± 3.5	5.3 ± 3.2
16.9-18.8	28.2 ± 2.6	10.6 ± 2.8	11.7 ± 3.5	97.3 ± 8.1	22.7 ± 4.7	6.8 ± 3.7
18.8-20.5	31.6 ± 3.7	11.7 ± 5.3	14.3 ± 4.6	104.2 ± 10.3	7.8 ± 4.7	9.9 ± 4.2
20.5-22.5	26.4 ± 2.8	13.7 ± 3.9	25.8 ± 3.2	115.3 ± 8.8	7.8 ± 4.7	9.9 ± 4.7
22.5-24.9	23.0 ± 2.4	6.8 ± 4.6	18.2 ± 5.4	87.7 ± 7.7		5.7 ± 4.4
24.9-26.9	16.5 ± 5.8			49.2 ± 7.5		
26.9-29.1	9.3 ± 6.0			41.9 ± 5.1		
29.1-31.7	10.6 ± 6.3			45.6 ± 6.2		
31.7-33.6	12.7 ± 8.1			26.7 ± 12.8		
33.6-35.7	11.9 ± 8.0			19.6 ± 7.8		
35.7-38.0	8.8 ± 7.9					

Table 7. Measured cross sections (in mb) for production of gamma rays following neutron interactions with  $^{59}\text{Co}$ 

$E_n$ (MeV)	Gamma-ray energy (keV)				
	1223.8	465.7	454.3	858.2	1166.3
7.75- 8.44			5.4 ± 3.0		
8.44- 9.23			4.8 ± 3.0		
9.23- 9.82			8.1 ± 3.8		
9.82-10.4			6.7 ± 3.8		
10.4 -11.1			4.6 ± 3.7		
11.1 -12.0			11.5 ± 1.1		
12.0 -12.9			12.2 ± 12.2		
12.9 -13.8			9.0 ± 3.5		
13.8 -15.2			8.6 ± 3.2		
15.2 -16.9			9.4 ± 1.1		
16.92-18.8			8.8 ± 3.5		
18.8 -20.5			7.3 ± 3.8		
20.5 -22.5		6.6 ± 4.4	8.2 ± 4.4	10.6 ± 5.1	
22.5 -24.9	15.9 ± 5.1	15.2 ± 17.3		11.1 ± 4.9	
24.9 -26.9	51.6 ± 5.3	22.3 ± 2.6		7.7 ± 6.1	7.9 ± 5.8
26.9 -29.1	64.4 ± 7.9	39.5 ± 4.0		9.0 ± 7.2	17.2 ± 6.6
29.1 -31.7	50.9 ± 9.6	50.1 ± 5.1		11.3 ± 7.0	13.1 ± 6.6
31.7 -33.6	92.7 ± 13.9	50.3 ± 7.3			13.7 ± 8.0
33.6 -35.7	53.3 ± 13.6	40.1 ± 7.3			9.2 ± 7.5
35.7 -38.0	39.8 ± 12.4	9.7 ± 6.9			

Table 8. Measured cross sections (in mb) for production of gamma rays following neutron interactions with  $^{59}\text{Co}$

$E_n$ (MeV)	Gamma-ray energy (keV)				
	472.7	810.5	1674.7	122.0	1061.3
4.49- 5.36	2.1 ± 2.0				
5.36- 6.19	3.8 ± 2.3				
6.19- 7.04	2.2 ± 2.4				
7.04- 7.75	3.0 ± 2.7				
7.75- 8.44	6.2 ± 3.0				
8.44- 9.23	7.7 ± 3.1				
9.23- 9.82	7.0 ± 4.7				
9.82-10.4	5.5 ± 3.8	4.5 ± 4.3			
10.4 -11.1	7.5 ± 3.8	10.6 ± 2.1			
11.1 -12.0	8.9 ± 3.8	32.0 ± 2.6			
12.0 -12.9	7.7 ± 3.7	14.9 ± 2.8			
12.9 -13.8	10.1 ± 3.5	41.9 ± 3.2			
13.8 -15.2	6.0 ± 3.1	47.7 ± 3.0			
15.2 -16.9	4.3 ± 3.1	66.1 ± 3.7	5.7 ± 3.1		
16.9 -18.8	4.9 ± 3.6	101.3 ± 6.9	8.3 ± 3.7	11.2 ± 3.2	
18.8 -20.5	6.5 ± 4.1	141.5 ± 11.9	8.1 ± 4.7	13.9 ± 3.7	
20.5 -22.5		145.2 ± 9.9	15.1 ± 4.4	13.7 ± 3.5	
22.5 -24.9		162.6 ± 0.9	7.8 ± 4.4	15.4 ± 3.5	
24.9 -26.9		146.2 ± 8.9	5.6 ± 5.0	19.8 ± 4.6	11.8 ± 5.8
26.9 -29.1		141.9 ± 9.9		35.2 ± 5.3	23.6 ± 3.4
29.1 -31.7		121.2 ± 10.8		35.7 ± 5.3	29.8 ± 4.3
31.7 -33.6		102.2 ± 18.1		33.1 ± 7.4	44.1 ± 7.7
33.6 -35.7		97.6 ± 11.7		24.6 ± 6.7	62.3 ± 12.0
35.7 -38.0		97.6 ± 16.6		20.4 ± 6.7	46.7 ± 8.6

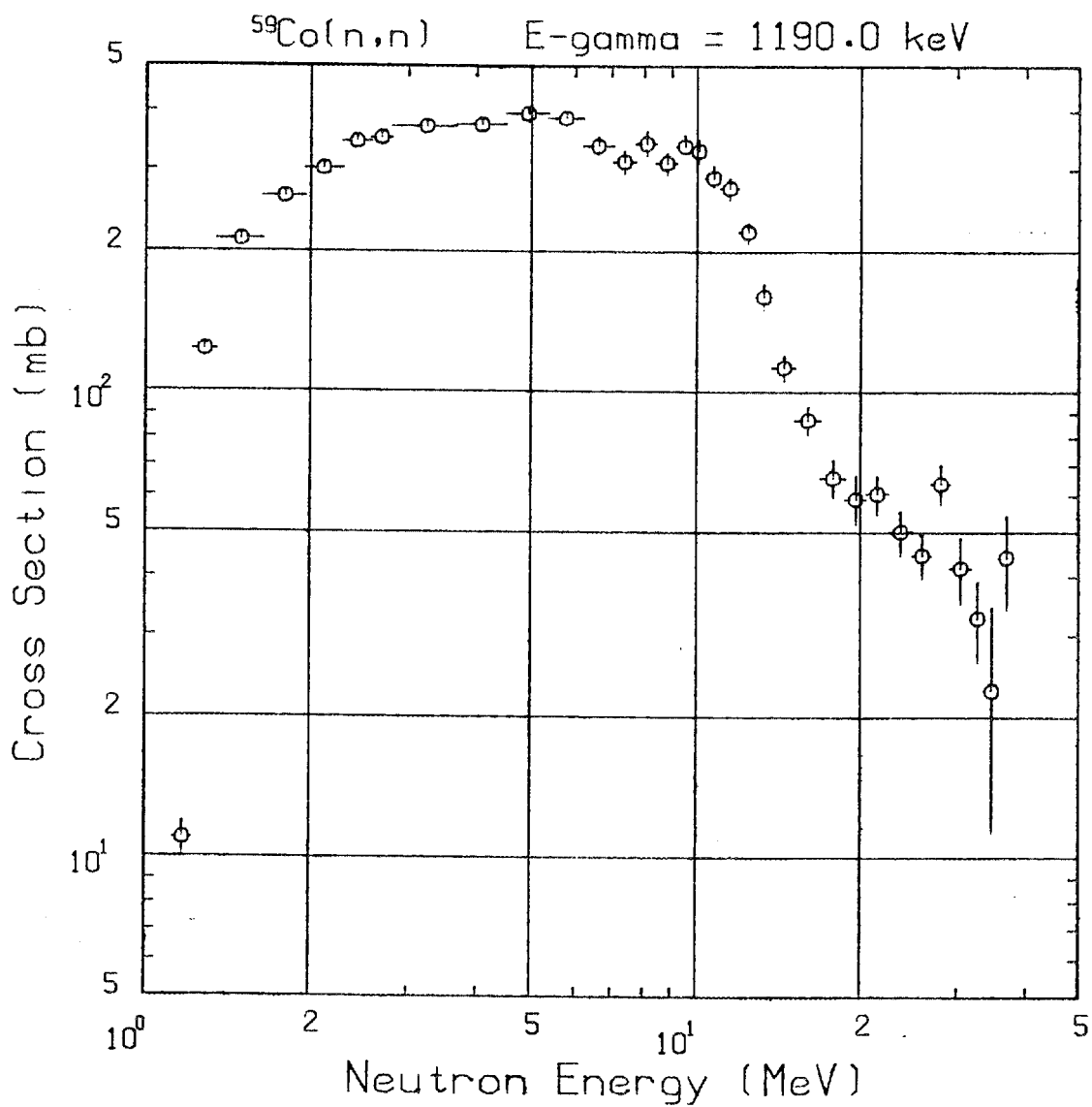


Fig. 5. A plot of the 1190.0-keV gamma-ray cross section for the  $(n,n')$  reaction for different incident neutron energies.

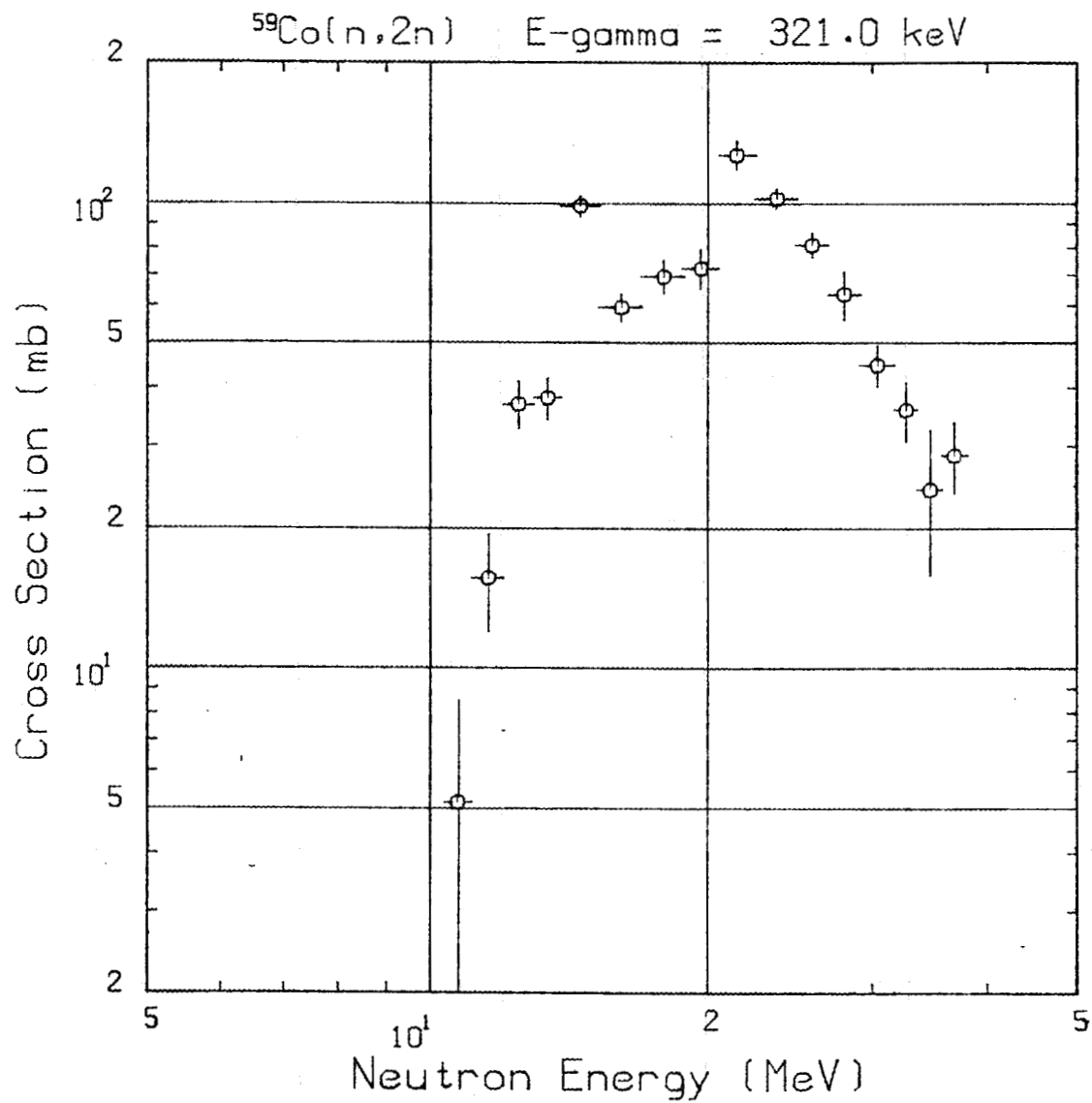


Fig. 6. A plot of the 321.0-keV gamma-ray cross section for the  $(n,2n)$  reaction for different incident neutron energies.

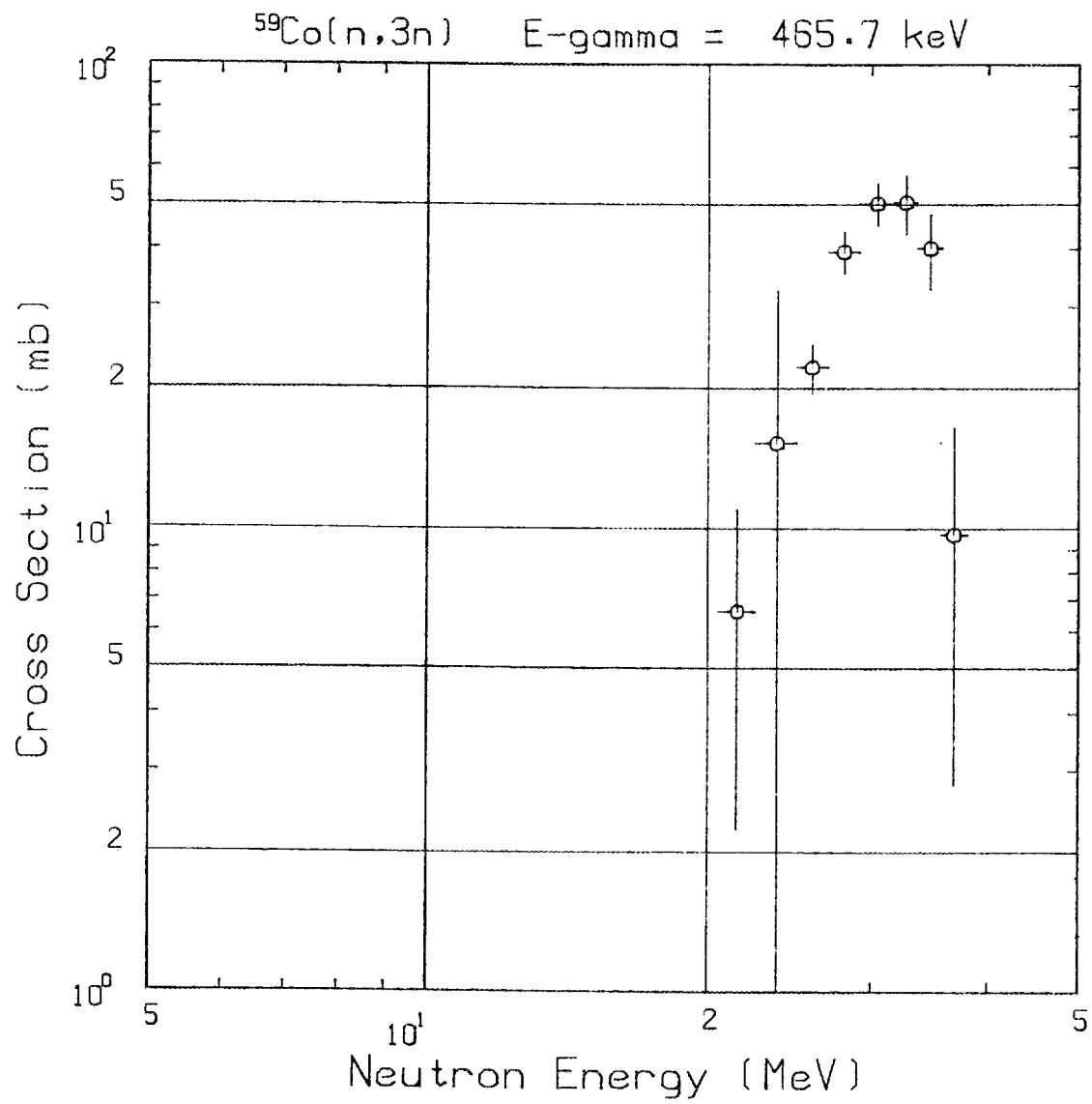


Fig. 7. A plot of the 465.7-keV gamma-ray cross section for the  $(n,3n)$  reaction for different incident neutron energies.

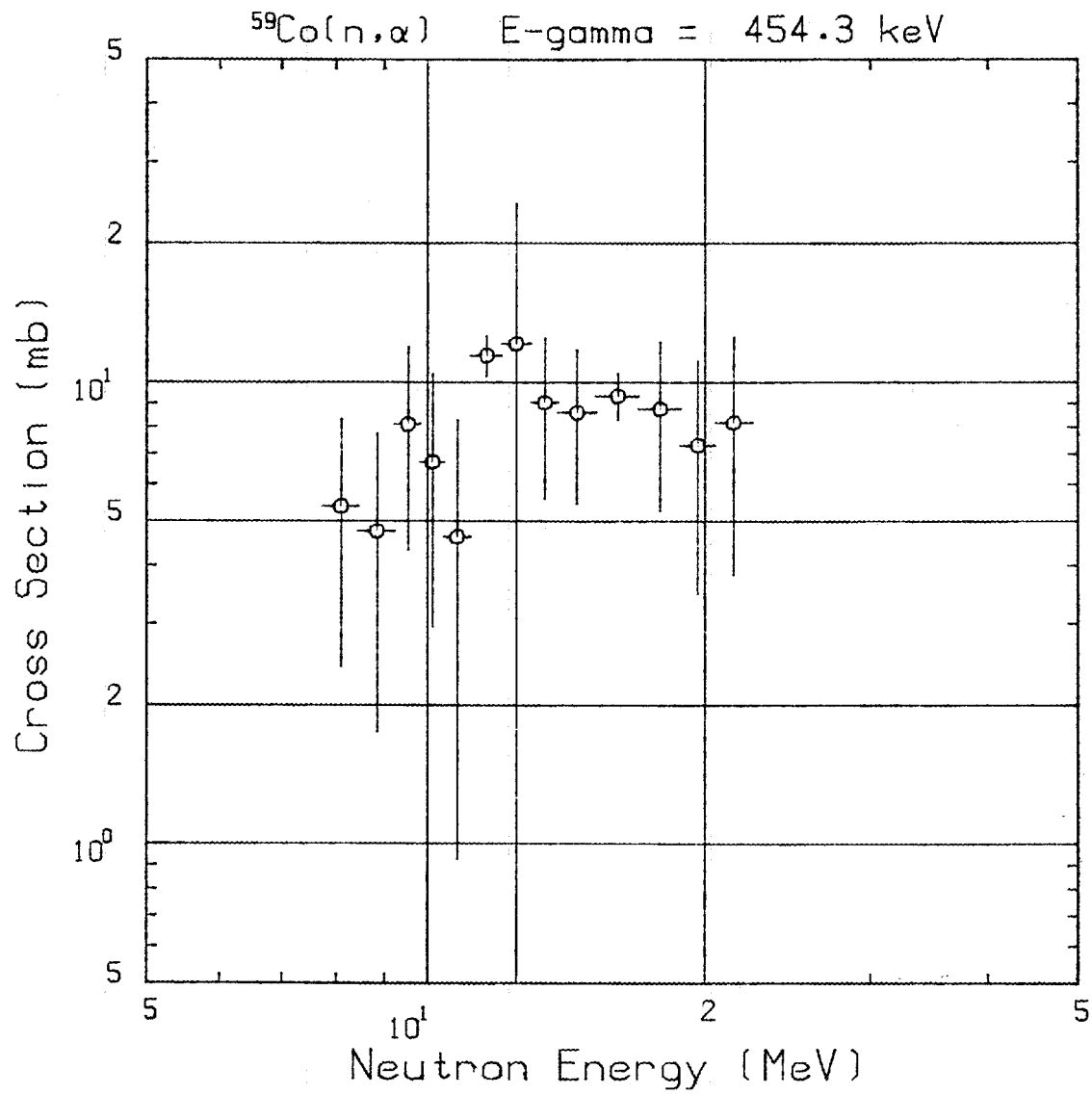


Fig. 8. A plot of the 454.3-keV gamma-ray cross section for the  $(n, ^4\text{He})$  reaction for different incident neutron energies.

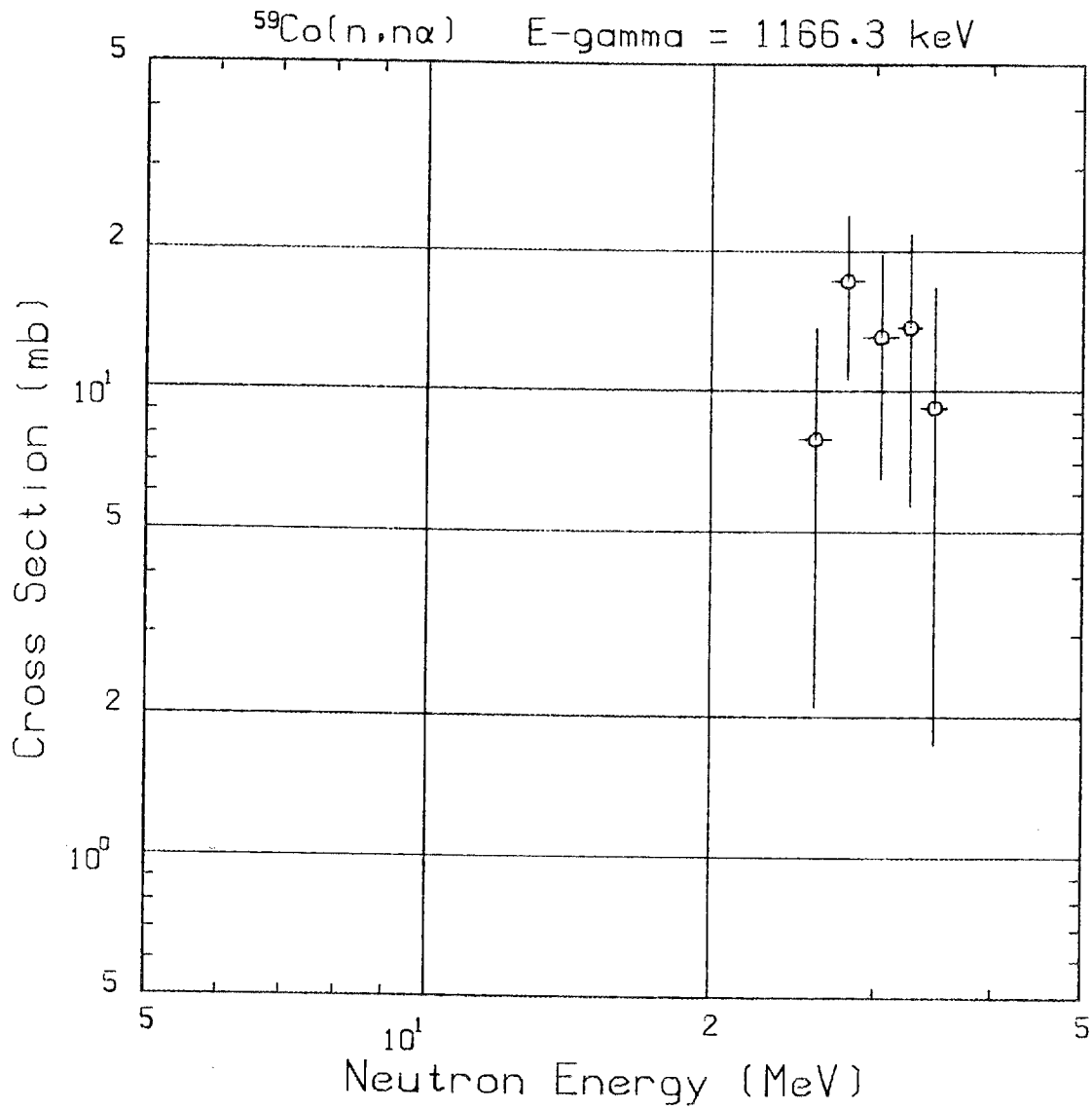


Fig. 9. A plot of the 1166.3-keV gamma-ray cross section for the  $(n, n^4\text{He})$  reaction for different incident neutron energies.

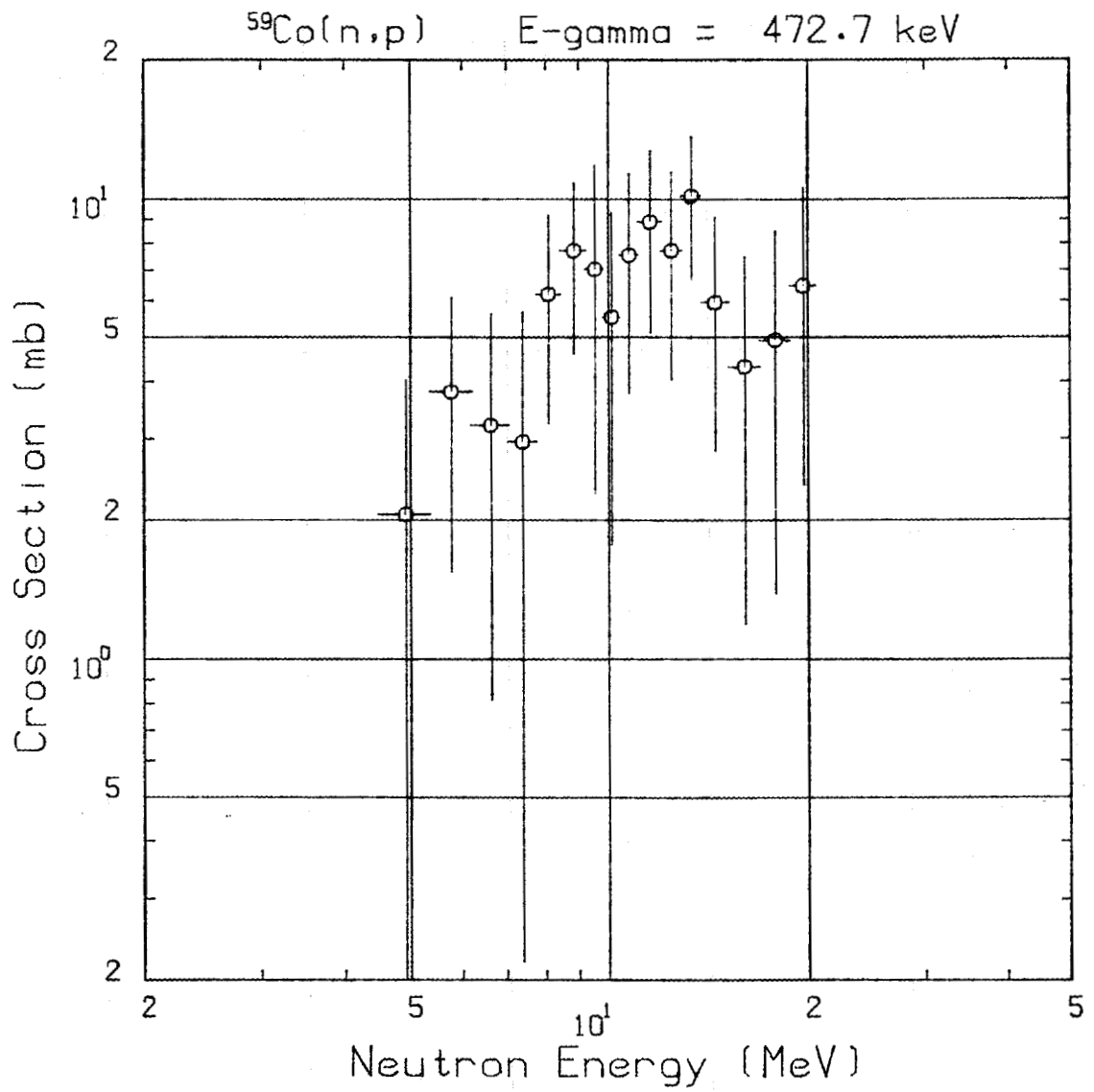


Fig. 10. A plot of the 472.7-keV gamma-ray cross section for the  $(n,p)$  reaction for different incident neutron energies.

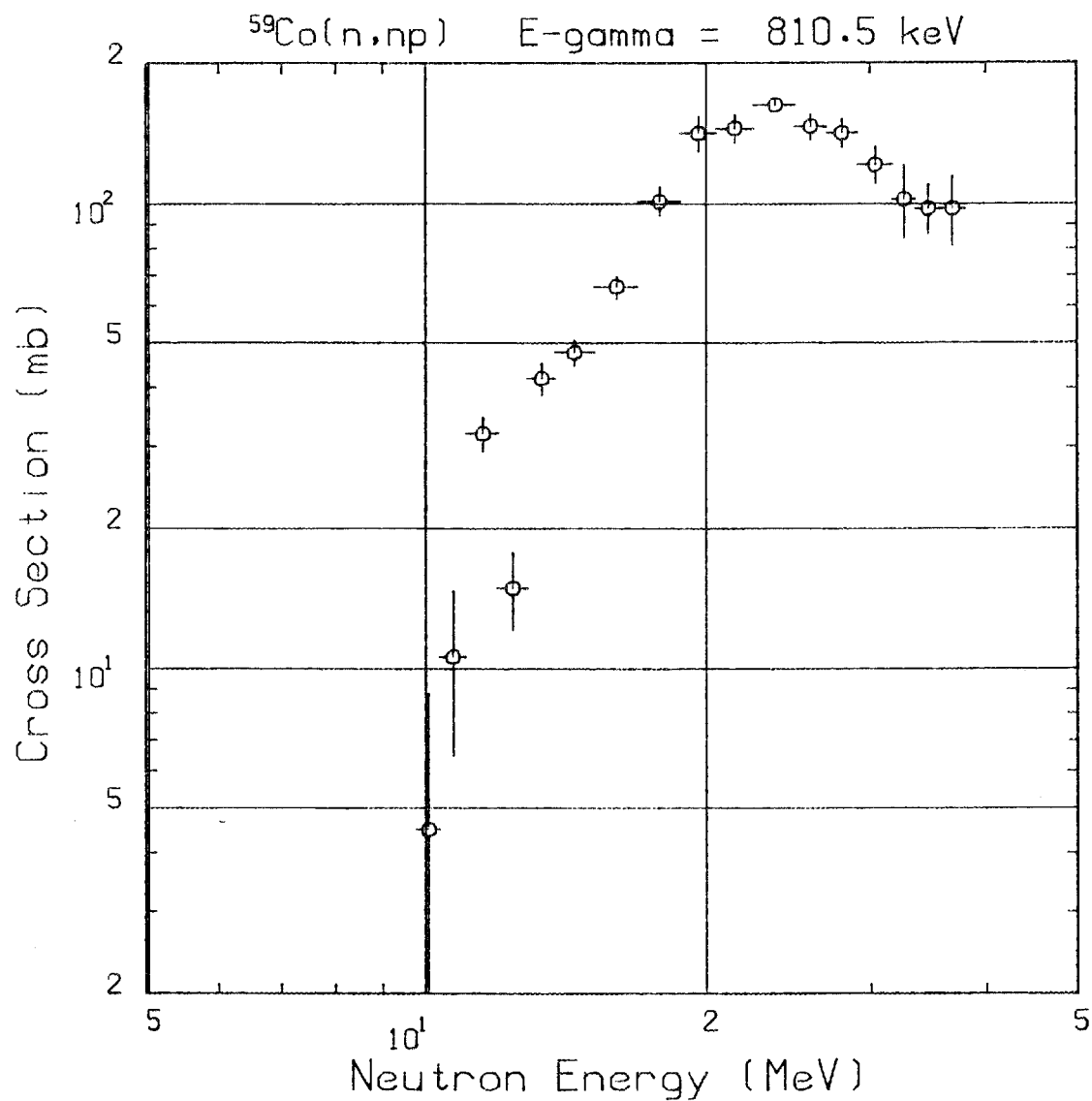


Fig. 11. A plot of the 810.5-keV gamma-ray cross section for the  $(n,np)$  reaction for different incident neutron energies.

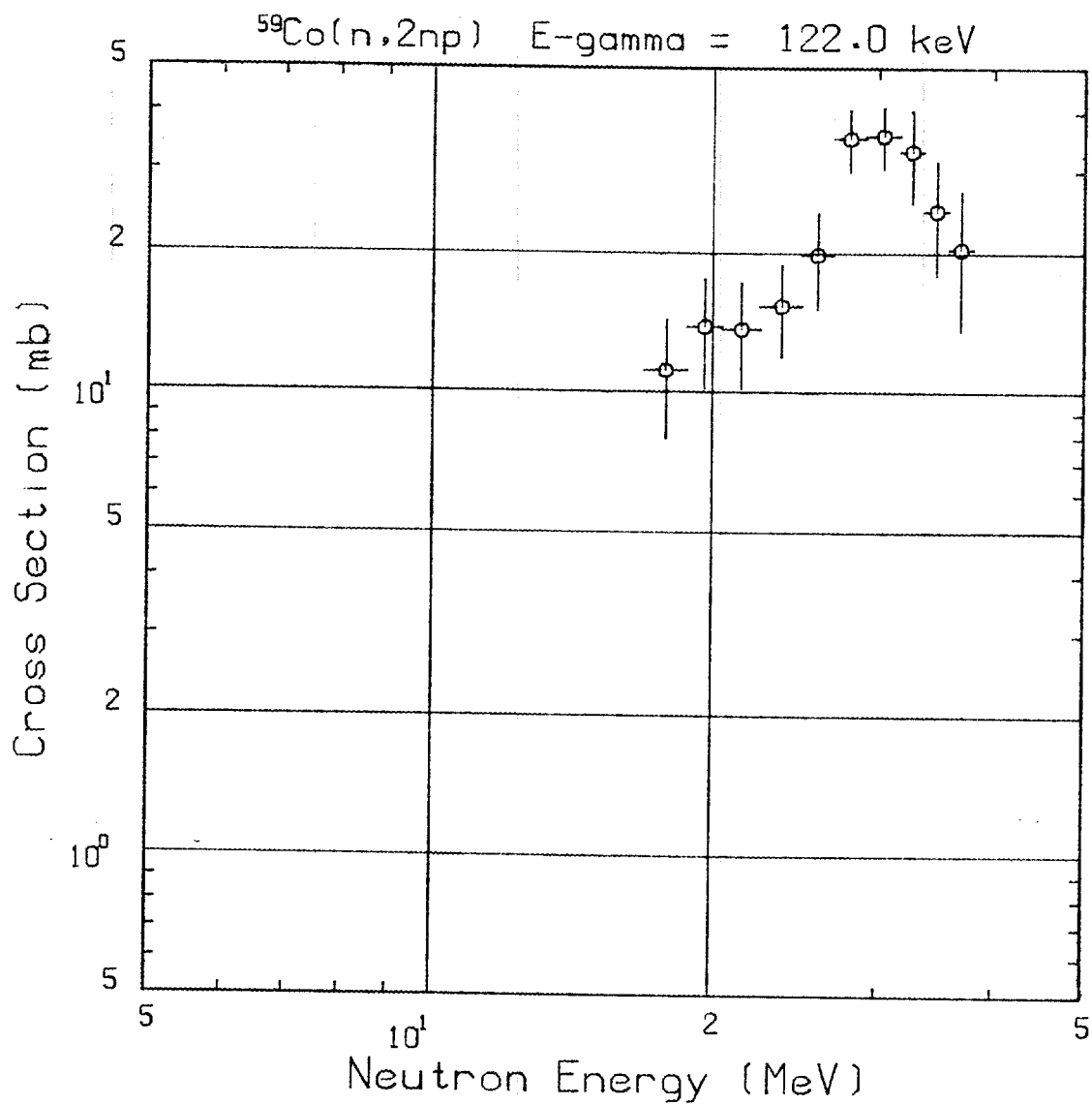


Fig. 12. A plot of the 122.0-keV gamma-ray cross section for the  $(n,2np)$  reaction for different incident neutron energies.

## 4. CONCLUDING REMARKS

The goal of the experiment, as discussed in the Introduction, is to present cross-section data for more accurate shielding calculations. This goal is well on its way to being met. The first task, that of obtaining peak yields, has been completed. The present results are of a preliminary nature, and further corrections are needed before these data are in final form. However, the present results do indicate relative probabilities for various reactions and should be useful in the interim for guidance in the study of neutron reactions with cobalt.

## REFERENCES

1. Z. W. Bell, J.K. Dickens, D. C. Larson, and J. H. Todd, *Nucl. Sci. and Eng.* **84**, 13 (1983).
2. J. K. Dickens and D. C. Larson, *Physical Review C* **39**, 1737 (1989).
3. GRPGLI (Gamma Ray Production Analysis Using Ge(Li) Detectors) was adapted by Z. W. Bell from TPASS code. J. K. Dickens, TPASS, *A Gamma Ray Spectrum Analysis and Isotope Identification Computer Code*, ORNL-5732, Oak Ridge National Laboratory (1982).
4. PLOTPACK, an IBM-PC BASIC program by R. L. Bywater, ORNL/TM-10191 (1986).
5. Table of Isotopes, edited by C. M. Lederer and V. S. Shirley, seventh edition (Wiley, New York, 1978).



## INTERNAL DISTRIBUTION

- |                       |   |
|-----------------------|---|
| 1. B. R. Appleton     | 24. J. H. Todd                          |
| 2-6. J. K. Dickens    | 25. B. A. Worley                        |
| 7. C. Y. Fu           | 26. J. J. Dorning consultant            |
| 8. J. A. Harvey       | 27. R. M. Haralick consultant           |
| 9. D. M. Hetrick      | 28. J. E. Leiss consultant              |
| 10-14. D. C. Larson   | 29. M. F. Wheeler consultant            |
| 15. R. L. Macklin     | 30. N. Moray consultant                 |
| 16. F. C. Maienschein | 31-32. Laboratory Records<br>Department |
| 17. M. J. Martin      | 33. Laboratory Records,<br>ORNL-RC      |
| 18. H. S. Payne       | 34. Document Reference<br>Section       |
| 19. R. W. Peelle      | 35. Central Research Library            |
| 20. F. G. Perey       | 36. ORNL Patent Section                 |
| 21. S. A. Raby        |   |
| 22. R. W. Roussin     |   |
| 23. R. R. Spencer     |   |

## EXTERNAL DISTRIBUTION

- 37-38. Office of the Assistant Manager for Energy Research and Development, U.S. Department of Energy, Oak Ridge Operations, P. O. Box 2001, Oak Ridge, TN 37831
39. Prof. Francis D. Correll, Department of Physics, U.S. Naval Academy, Annapolis, MD 21402-5026
40. Robert J. Howerton, Lawrence Livermore National Laboratory, C.P. Division, L-298, P. O. Box 808, Livermore, CA 94550
41. National Nuclear Data Center, Brookhaven National Laboratory, Upton, NY 11973
42. D. L. Smith, Engineering Physics Division, Bldg. 314, Argonne National Laboratory, Argonne, IL 60439
- 43-45. Thomas E. Slusarchyk, 10620 Fairpine Dr., Pensacola, FL 32506
46. O. A. Wasson, National Institute of Standards and Technology, B111, Radp Bldg., Gaithersburg, MD 20899
47. Phillip G. Young, T-2, MS B243, Los Alamos National Laboratory, Los Alamos, NM 87545
- 48-57. Office of Scientific and Technical Information, P. O. Box 62, Oak Ridge, TN 37831